

Similarity in longitudinal decays of free jump and submerged jump

S. Choi & S.-U. Choi

Department of Civil and Environmental Engineering, Yonsei University, Seoul, Korea

ABSTRACT: Both free jump and submerged jump are of importance in practical engineering. The free jump is known to dissipate the kinetic energy most efficiently. The submerged jump, which is an alternative of the free jump, dissipates the kinetic energy over an elongated length of the roller with less pressure fluctuations on the bed. This study presents numerical simulations of hydraulic jumps of flows over an embankment-type weir to investigate the similarity of decaying flow structures for the free jump and submerged jump. The URANS equations are solved with the $k-\omega$ SST turbulence model with the VOF method for computing the multiphase flow of air-water mixtures. The numerical model is validated against laboratory experiments, showing moderate agreement. Simulation results reveal that the mean velocity, turbulence intensity, and Reynolds stress for the free jump decay fast in the longitudinal direction compared with the submerged jump.

1 INTRODUCTION

The low head embankment-type weirs are very common in Korea. The number of this type of weirs is over 34,000. Previously, the apron of these weirs was not long enough for the hydraulic jump to take place within its range. Therefore, the stream bed has frequently been exposed to the severe scour downstream from the weir, which resulted in the destruction of the weir in the worst case. This led the recent change of the design specification for the apron length of the low head embankment-type weir.

Flows over an embankment-type weir exhibit various flow regimes. For low flows, a free jump occurs downstream from the weir. If the tailwater level increases, then the hydraulic jump moves upstream. If the free jump takes place at the toe of an embankment-type weir, then the jump is called optimum jump. The optimum jump is named because the efficiency of energy dissipation is best. It also requires the minimum distance for dissipating the energy. If the tailwater level increases further, then the submerged jump occurs. The submerged jump dissipates less energy due to the decreased jet mixing, compared with the free jump. This becomes pronounced as the degree of submergence increases. However, the roller of the submerged jump, over which the energy dissipates, is elongated considerably.

This study investigates numerically the similarity in the longitudinal decays of the free jump and submerged jump. For the numerical simulations, 2D Unsteady Reynolds-Averaged Navier-Stokes (URANS) equations are solved with the $k-\omega$ SST turbulence model. The volume of fluid (VOF) method is used to track the free surface and to compute the water-air multiphase flow. Model validation is carried out for both free jump and submerged jump by comparing computed vertical structures with measured data obtained in the literature.

Using the computed results, the flow structures, such as the streamwise mean velocity, turbulence intensity, and Reynolds stress are obtained and their decays in the longitudinal direction are

estimated. It is found that the longitudinal decays of the flow structures for the free jump are not similar to those for the submerged jump.

2 NUMERICAL MODEL

2.1 Governing equations

The following URANS equations are solved to compute the flows over the weir:

$$\frac{\partial \rho}{\partial t} + \frac{\partial \rho \tilde{u}_i}{\partial x_i} = 0 \quad (1)$$

$$\frac{\partial \rho \tilde{u}_i}{\partial t} + \frac{\partial \rho \tilde{u}_i \tilde{u}_j}{\partial x_j} = -\frac{\partial \tilde{p}}{\partial x_i} + \frac{1}{\partial x_j} \left\{ (\mu + \mu_t) \frac{\partial \tilde{u}_i}{\partial x_j} \right\} + \rho g_i \quad (2)$$

where x_i is the Cartesian axis direction ($i = 1, 2$), \tilde{u}_i is the ensemble-averaged velocity in the x_i direction, t is the time, ρ is the density of the water-air mixture, \tilde{p} is the ensemble-averaged pressure, μ is the viscosity of the water-air mixture, μ_t is the turbulent viscosity, and g is the gravitational acceleration. In the present study, the VOF method is used to compute the free surface (Hirt and Nichols, 1981).

2.2 Turbulence model

The k - ω SST turbulence model proposed by Menter (1992) is used to estimate the turbulent viscosity μ_t in Eq.(2). That is,

$$\mu_t = \frac{a_1 \rho k}{\max(a_1 \omega, \bar{S} F_2)} \quad (3)$$

where k is the turbulence kinetic energy, ω is the specific dissipation rate of k , \bar{S} is the strain rate of the flow, α_1 is a model constant ($= 0.31$), and F_2 is a blending function. In the present study, the blending function proposed by Menter (1992) is used. To obtain k and ω , the transport equations for k and ω are solved with model coefficients in Menter (1992).

As for boundary conditions, the streamwise mean velocity from the log-law is prescribed with the upstream flow depth at the inlet boundary, and the pressure is set to be hydrostatic with arbitrary small values for k and ω at the inlet boundary. The outlet boundary is a freefall, where the ensemble-averaged pressure is zero. The no-slip boundary condition is used at the wall. At the air-filled upper boundary of the solution domain, the ensemble-averaged pressure is set to zero.

3 APPLICATION

The flow conditions in Fritz and Hager's (1998) experiments are used to simulate the free jump and submerged jumps numerically. The unit discharge, water depth of approach flow, length of weir crest, and height of weir are 0.055 m²/s, 0.4 m, 0.3 m, and 0.3 m, respectively. The flow condition and the dimension of the weir result in a relative embankment length of 0.25, indicating a broad-crested weir. For a fixed unit discharge, a free jump and submerged jumps are reproduced by varying the tailwater depth. For the submerged jumps, the submergence factor S ranges between 0.5 and 0.88.

Figure 1(a) and 1(b) show the distributions of the streamwise mean velocity at various longitudinal distances for the free jump and submerged jump for $S = 0.77$, respectively. In the figure, the computed results are compared with the measured data in Fritz and Hager (1998). The interface of the roller and the free surface are also plotted in the figure.

For both free jump and submerged jump, the numerical model accurately predicts the two flow regimes that consist of recirculating flows over the wall-jet-like flow in the developed zone. The computed roller length for the submerged jump with $S = 0.77$ appears to be 2.2 times longer than that for the free jump. Interestingly, the roller length predicted by the numerical model is longer

and shorter than the measured data for the free jump and submerged jump, respectively. Specifically, the computed roller length is 1.07 times longer than the measured data for the free jump, but 1.09 times shorter for the submerged jump. Compared with the velocity profile of the free jump, the velocity maximum for the submerged jump occurs in the vicinity quite close to the bed, resulting in a profile similar to that of the wall jet. This is because of the lower level of the adverse pressure gradient.

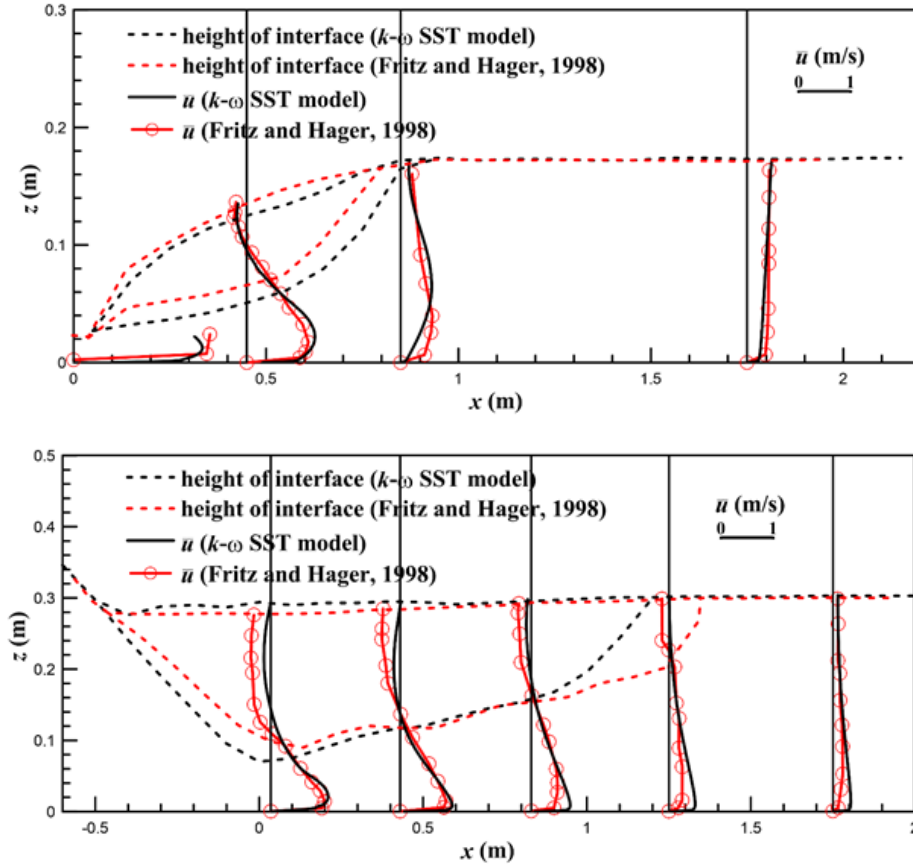


Figure 1. distribution of streamwise mean velocity

4 SIMILARITY

Figure 2(a) and 2(b) show the longitudinal decays of the peak streamwise mean velocity and turbulence intensity with distance, respectively, for the free jump and submerged jumps. Here, L_r and L_r' are the roller length for the free jump and the roller length from the origin for the submerged jump, respectively. The measured data for the free jump and for the submerged jumps are also plotted in the figure. Moderate agreement between the computed results and the measured data is observed in the figure.

As shown in the figure, the decay of the peak streamwise mean velocity for the free jump appears to be similar to that for the submerged jumps for $x/L_r \leq 0.7$. However, for $x/L_r > 0.7$, the decay of the submerged jumps is retarded, compared to that for the free jump. For the peak turbulence intensity, the decay of the free jump is accelerated for $x/L_r \leq 0.5$, but is slowed down afterwards, compared to the decay of the submerged jumps. In summary, the decays of the peak streamwise mean velocity and peak turbulence intensity for the free jump are not similar to those for the submerged jumps. This is not consistent with Fritz and Hager's (1998) finding that the peak streamwise mean velocity for both the free jump and the submerged jumps decay similarly. This may be due to that Fritz and Hager (1998) focused on the decay only in the developed zone. However, interestingly, the decays of the submerged jumps are similar regardless of the submergence factor.

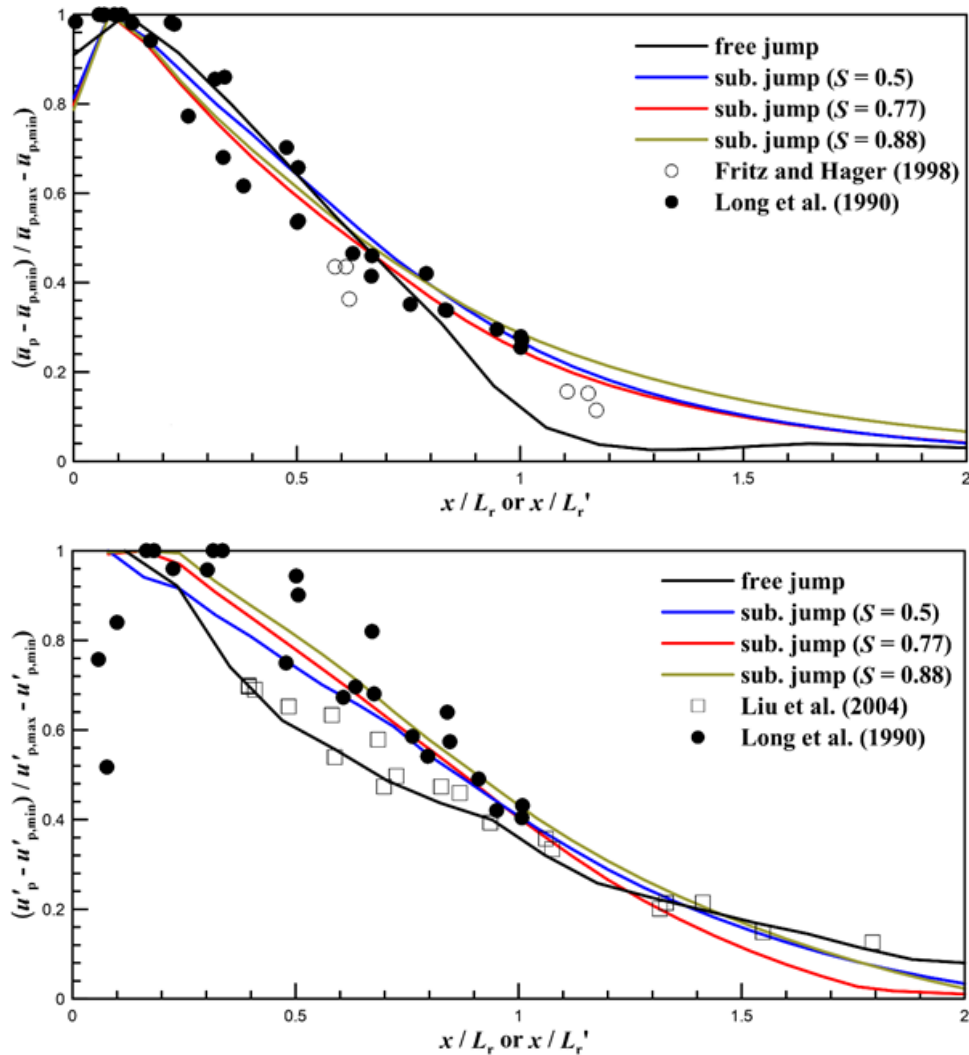


Figure 2. Longitudinal change in flow structures

5 CONCLUSIONS

This study investigated numerically the similarity of decaying flow structures for the free jump and submerged jumps. For numerical simulations, the URANS equations were solved with the $k-\omega$ SST turbulence model. The VOF method was used to compute the two-phase flow of air-water mixtures, and hydraulic jumps over an embankment-type weir were reproduced.

The numerical model was validated against the laboratory experiment by Fritz and Hager (1998). It was found that the numerical model predicts the roller length and distribution of mean velocity moderately for both free jump and submerged jump.

Finally, the similarity of longitudinally decaying flow structures, such as mean velocity and turbulence intensity, were presented. The decaying patterns of the turbulence intensity and Reynolds stress (although not presented here) for the free jump appeared to be different from those for submerged jumps. The longitudinal decay of the mean velocity for the free jump was similar to that for the submerged jump in the developed zone, but the free jump showed a different decaying pattern afterwards.

ACKNOWLEDGEMENT

This study was supported by the National Research Foundation of Korea (NRF) grant funded by the Korea Government (NRF2020R1A2B5B01098937).

REFERECNCES

- Fritz, H. M. & Hager, W. H. 1998. Hydraulics of embankment weirs. *Journal of Hydraulic Engineering* 124(9): 963-971.
- Hager, W. H. 1992. Energy dissipators and hydraulic jump. *Water science of technology library*, Vol. 8: 67–75. Dordrecht: Kluwer.
- Hirt, C. W. & Nichols, B. D. 1981. Volume of fluid (VOF) method for the dynamics of free boundaries. *Journal of Computational Physics* 39(1): 201–225.
- Jasak, H. 2009. OpenFOAM: Open source CFD in research and industry. *International Journal of Naval Architecture and Ocean Engineering* 1(2): 88-94.
- Liu M., Rajaratnam, N., & Zhu, D. Z. 2004. Turbulence structure of hydraulic jumps of low Froude numbers. *Journal of Hydraulic Engineering* 130(6): 511-520.
- Long, D., Steffler, P. M., & Rajaratnam, N. 1990. LDA study of flow structure in submerged hydraulic jump. *Journal of Hydraulic Research* 28(4): 437-460.
- Long, D., Steffler, P. M., & Rajaratnam, N. 1991. A numerical study of submerged hydraulic jumps. *Journal of Hydraulic Research* 29(3): 293-308.
- Ma, F., Hou, Y., & Prinos, P. 2001. Numerical calculation of submerged hydraulic jumps. *Journal of Hydraulic Research* 39(5): 493-503.
- Menter, F. R. 1992. *Improved two-equation k-omega turbulence models for aerodynamic flows*. NASA Ames Research Center, Moffett Field, CA.
- Van Leer, B. 1974. Towards the ultimate conservative difference scheme. II. Monotonicity and conservation combined in a second-order scheme. *Journal of Computational Physics* 14(4): 361-370.